

G. D. Ferney

S. L. Folkman

Department of Mechanical and  
Aerospace Engineering  
Utah State University  
Logan, UT 84322

---

# Development of a Method for Characterizing Joint Stiffness, Deadband, and Hysteresis

*This article documents the development of a procedure for characterizing the stiffness, deadband, and hysteretic behavior of struts with pinned joints. A test setup utilized procedures recommended by other authors. The test results included a calibration specimen with linear stiffness and near zero hysteretic behavior that identified the capabilities and limitations of the procedure. Tension/compression pull tests of the truss joints were conducted. The load vs. displacement curves showed stiffness, deadband, and hysteresis loops consistent with theory. Vibration damping was inferred from the hysteresis loops and compared with measured data from a three bay truss. © 1995 John Wiley & Sons, Inc.*

---

## INTRODUCTION

Many space structures currently being designed utilize deployable truss structures that can be compactly stored and easily deployed to their final configuration. A clevis and tang pinned joint is a logical consideration for a deployable truss because rotation about the pin axis is not restrained. An ideal joint design might be described as one with constant stiffness throughout the operating load range along with negligible deadband and hysteresis. Unfortunately, typical clevis/tang designs exhibit different stiffness in tension and compression. Deadband and hysteresis are generally observed unless preloads can be applied to prevent gaps from occurring in the clevis/tang/pin interface.

Truss dynamics are significantly influenced by joint deadband and hysteresis. Joints typically provide the greatest source of passive damping in

most structures without damping materials or treatments (Plunkett, 1980). Truss structures using pinned joints can have very high damping rates. Damping has been shown to be dependent on vibration amplitude and gravity load (Folkman and Redd, 1990). Pin gaps have been attributed to driving higher modes with nonlinear results (Hayasaka et al., 1992).

Peebles and Kempster (1988) evaluated candidate space station truss joints for their stiffness and damping characteristics. The joint stiffness and loss factors were reported. Because of the tight fitting design of the joints and the larger preload of 1,334 Newton (N), very little hysteretic behavior was observed at load levels of 445–2,224 N. Crawley, Sigler, and van Schoor (1988) reported analytical and experimental techniques to predict and verify the damping of flexible space structures. Their results show that predicting damping from hysteresis tests is promising,

---

Received August 18, 1994; Accepted January 27, 1995.

Shock and Vibration, Vol. 2, No. 4, pp. 289–295 (1995)  
© 1995 John Wiley & Sons, Inc.

CCC 1070-9622/95/040289-07

even though the method only showed a general correlation at best. All of the above investigations used a securely fastened strut joint where all strut rotations were restrained. No tension/compression tests on struts using pinned joints were found.

The nonlinearities introduced by deadband and hysteresis dramatically complicate structural design and analysis. Because analytical estimates of deadband and hysteretic behavior are at best difficult, measurement of strut characteristics is important. Modeling truss structures using pinned joints requires accurate knowledge of the joint load vs. displacement response. Methods for accurate characterization of strut stiffness, deadband, and hysteresis are needed. Potential problem areas include:

1. removing load cell deadband;
2. applying compressive loads while preventing buckling motions at the pin location;
3. selection of displacement transducers with high sensitivity;
4. removing bending motions from the displacement reading;
5. minimizing applied bending moments; and
6. calibration of the test setup.

Because the test setup described in this article is focused on a quasistatic procedure, it is recognized that dynamic characterization of struts is also needed. A force-state-mapping technique has received considerable attention (Masters and Crawley, 1993). A basic problem in all of these procedures is calibration of results. Quasistatic test results should be comparable with low frequency force-state-mapping results and provide a check on procedures. It is hoped that the method reported here provides complimentary support to force-state-mapping techniques.

## BASIC CONCEPTS

In the investigation of structural damping, loss factor and logarithmic decrement are parameters frequently used to quantify damping phenomena. Loss factor,  $\eta$ , is the quantity used in relating hysteretic behavior to damping. In a quasi-linear system, it can be calculated from a load vs. displacement response curve using

$$\eta = \frac{\Delta U}{2\pi U_{\max}} \quad (1)$$

where  $\Delta U$  is the energy dissipated per cycle and  $U_{\max}$  is the peak strain energy or the energy stored per cycle. Crawley et al. (1988) report that for built-up structures, an overall loss factor,  $\eta_t$ , can be given by

$$\eta_t = \frac{\sum_{i=1}^n \Delta U_i}{2\pi \sum_{i=1}^n U_i} \quad (2)$$

where  $\Delta U_i$  is the energy dissipated in element  $i$  and  $U_i$  is the energy stored in element  $i$ .

By recording the oscillation decay of a system, the logarithmic decrement  $\delta$ , can be used to relate the decay of peak amplitudes to damping according to the relationship

$$\delta = \frac{1}{n} \ln \left( \frac{A_0}{A_n} \right) \quad (3)$$

where  $n$  is the number of cycles,  $A_0$  is the initial peak amplitude and  $A_n$  is the peak amplitude after  $n$  cycles. A linear system with light damping exhibits the following relationship between  $\delta$  and  $\eta$  (Hutton, 1981).

$$\eta = \frac{\delta}{\pi} \quad (4)$$

## TEST SPECIMEN

A three bay truss was constructed. The individual truss struts consisted of a section of tubing

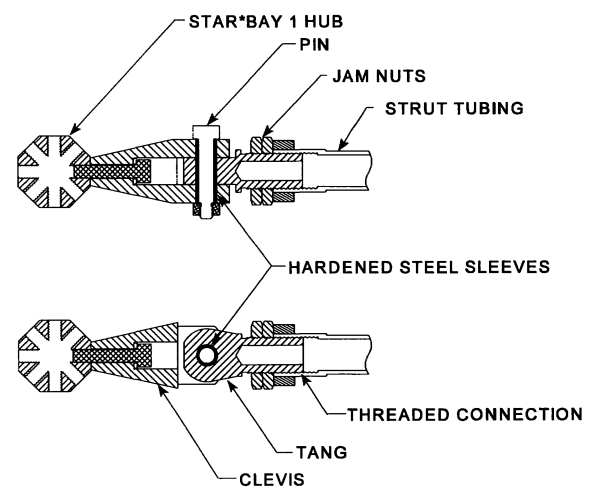


**FIGURE 1** Illustration of the tang and clevis joint design.

with pinned joints on each end as illustrated in Figure 1. The tubing acted like a turnbuckle because right- and left-handed threads were used to connect the pinned joints at the ends. Precision machined shoulder bolts were used as the joint pin with sizes ranging from 4.534 to 4.737 mm. The joint can be locked to prevent deadband and rotation about the pin. The locked configuration was obtained by placing shims between the clevis and tang pieces and by tightening the shoulder bolt. Thus, a large preload was applied across the clevis/tang interface to lock the joint.

**EXPERIMENT DESCRIPTION**

The experiment setup is illustrated in Figure 2. During hysteresis tests, a pinned joint was subjected to cyclic tension/compression loading. Tensile testing equipment provided the cyclic tensile load and three springs in parallel provided a compressive preload. A compliant link placed in the load path allowed the cyclic tensile load to be applied in a very smooth, controlled fashion. A cyclic tensile load of 133–667 N coupled with a compressive preload of 400 N resulted in a  $\pm 267$  N cycle applied to the test specimen. A load cell provided the in-line tensile load measurement during testing. Three linear variable displacement transducers (LVDTs) were mounted 120° apart and used to measure displacement of the test specimen. By averaging the three displacement signals, any rotation or bending in the strut was removed from the measurement. The dis-

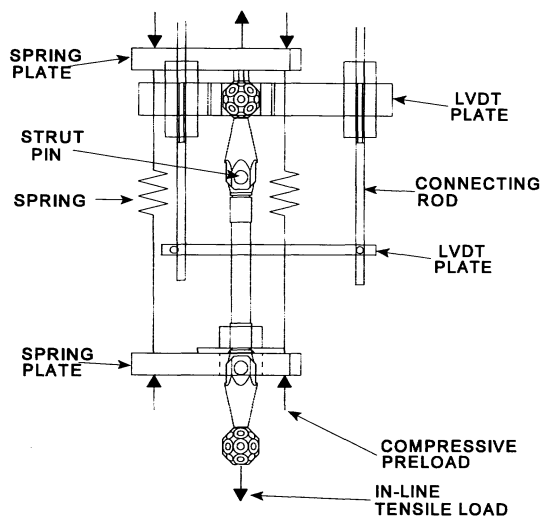


**FIGURE 2** Illustration of the test fixture.

placement and load data were recorded using an integrating voltmeter to help remove 60 Hz electrical noise.

To conduct a hysteresis test, the test fixture is placed in-line with the load cell and the compliant member. An initial tensile load was applied to ensure that the joint would remain stable during application of the compressive preload. The springs were then incrementally stretched to apply the compressive preload. With the fixture installed and the LVDTs adjusted, the tensile testing machine was set to cycle within the minimum and maximum values of tensile load. The three LVDTs and load cell voltages were recorded. The LVDT readings were later averaged to provide a measure of in-line axial displacement.

**SETUP CALIBRATION**

A section of aluminum tubing was installed in the fixture for a tension/compression reference test. The calibration was necessary to determine the capabilities and limitations of the setup. The LVDT plates were mounted on the tubing at reference lengths of 95.25 and 108 mm. Figure 3 illustrates the load vs. displacement curves. To determine the slope or stiffness, a first-order least-squares curve fit was calculated for the measured data. The stiffness of the tubing was measured at 21.9 and 24.3 kN/mm, which is within 3% of predicted values. The method adequately measured the stiffness characteristics of the section of aluminum tubing specimen.

The horizontal variations in the two curves in Figure 3 indicate the presence of noise in the displacement measurement. A loss factor of 0.01

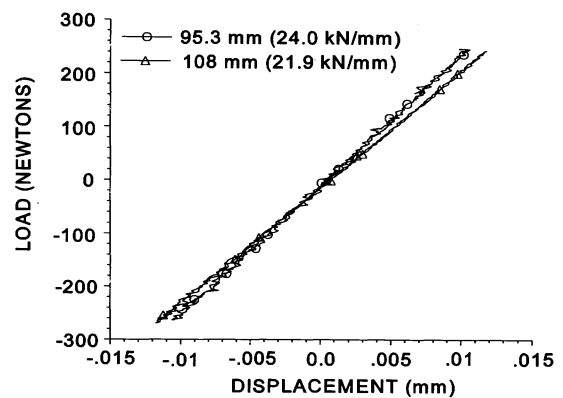


**FIGURE 3** Plot of the hysteresis test of aluminum tubing.

is calculated from the raw data. This loss factor value is inaccurate due to the noise in the displacement data. Cold rolled aluminum should exhibit a loss factor closer to 0.0004 (Steidel, 1971). Thus, this method is inadequate for measuring material damping. However, the information represents a baseline reference of the capability of the experiment setup to measure hysteresis. The above results do imply that a loss factor of 0.01 would be representative of a lower limit of the system.

**EXPERIMENT RESULTS**

A truss strut was tested in tension and compression to characterize the hysteretic behavior of the load vs. displacement relationship. Figure 4 illustrates the hysteresis loops for pin sizes from 4.534 to 4.712 mm. The hysteretic behavior is very apparent in the load vs. displacement curves. The test of the 4.534-mm pin shows a spike as the cycle leaves the positive tensile load. The spike is attributed to sudden realignment of the fixture due to the large joint gap.

Figure 5 shows the variation of hysteresis loops with pin diameters ranging from 4.712 to 4.737 mm. Larger pins reduce joint gap and produce decreases in deadband. Between the sizes of 4.729 and 4.735 mm, the shape of the hysteresis curve changed indicating that joint alignment was taking place and that joint gap was very small. The inside diameter of the tange and clevis portions of the joint is 4.740 mm.

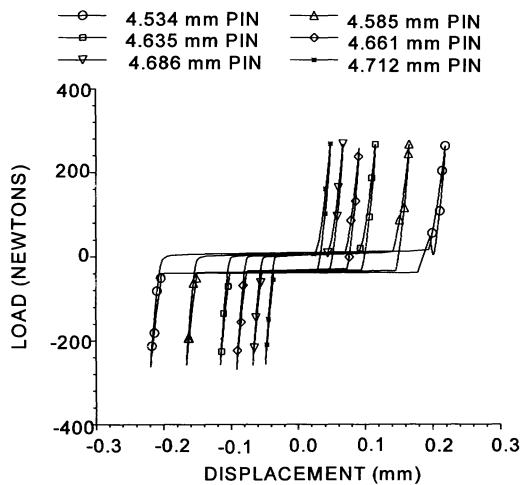


**FIGURE 4** Plot of hysteresis tests for pins ranging from 4.534 to 4.712 mm diameter.

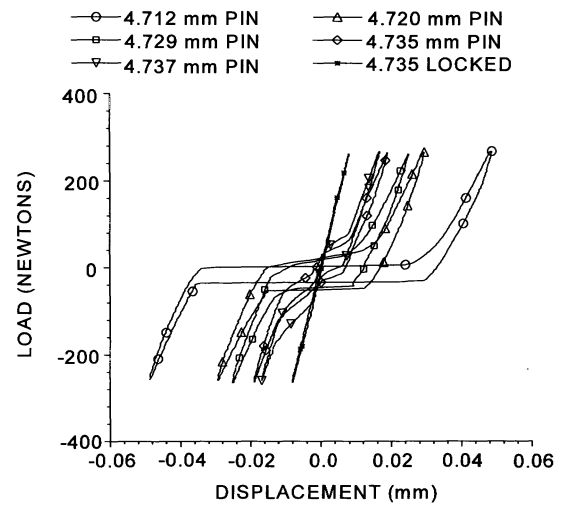


**FIGURE 5** Plot of hysteresis tests for pins ranging from 4.712 to 4.737 mm diameter.

The resulting load vs. displacement relationship was analyzed to determine strut stiffness in tension and compression, strut deadband, and strut hysteresis characteristics. The stiffness was computed with a linear least-squares fit of the 25 points prior to the minimum and maximum load peaks in the cycle. The stiffness of each joint varies in tension and compression as expected (see Fig. 6). As the pin size increases, the tensile and compressive stiffness values tend to increase.

The hysteresis characteristics were computed by integrating the loop area and dividing by the peak strain energy. Figure 7 illustrates the rela-

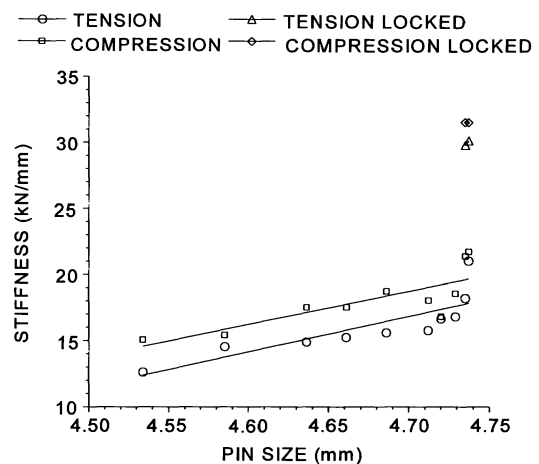


**FIGURE 6** Plot of joint stiffness in tension and compression as a function of pin size.

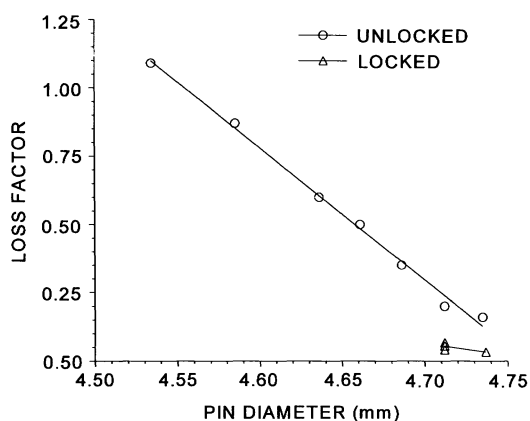


**FIGURE 7** Plot of joint loss factor as a function of pin size.

relationship between loss factor and pin size. Loss factor decreases as pin size increases because the joint gap or deadband also decreases. Locked joints showed much smaller loss factors and much higher stiffness than the unlocked joints.

**OBSERVED PHENOMENA**

For a 4.737-mm pin, the slope and general shape of the curve (see Fig. 8) deviates significantly from the idealized pinned joint curve. The joint appeared to experience some joint realignment while moving through the deadband. A larger than expected hysteresis loop was obtained indicating that significant friction forces must have been present.

To investigate these phenomena, lateral movement of the joint was monitored using two dial indicators. Figure 9 defines the *x* and *y* mea-

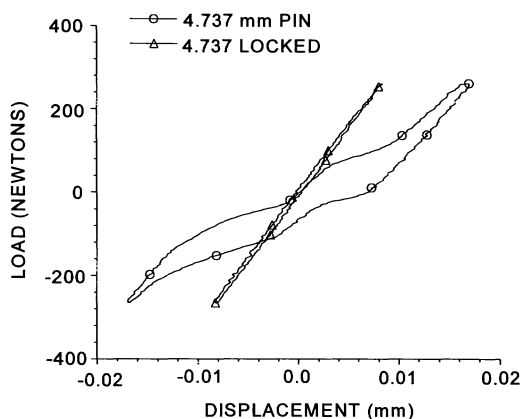


**FIGURE 8** Plot of hysteresis test for 4.737-mm pin.

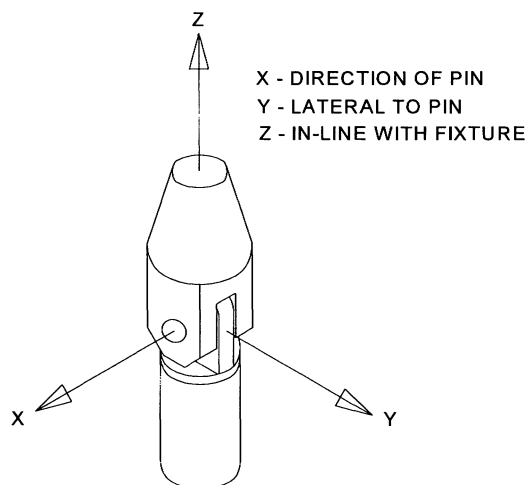


**FIGURE 9** Illustration of the off axis directions used to describe joint movements.

surement directions with respect to the joint. Figure 10 illustrates the recorded values at several points along the load path. Although significant motion occurred throughout the entire cycle, most of the lateral motion occurred in the deadband region. Misalignment due to imprecision in the pin/clevis/tang interface is suspected to be the cause of these movements. As the joint changed alignment, friction forces could have caused the large hysteresis loops observed.

**COMPARISON WITH LOGARITHMIC DECREMENT TESTING**

The strut loss factors were utilized to predict a loss factor for the entire three bay truss. To use

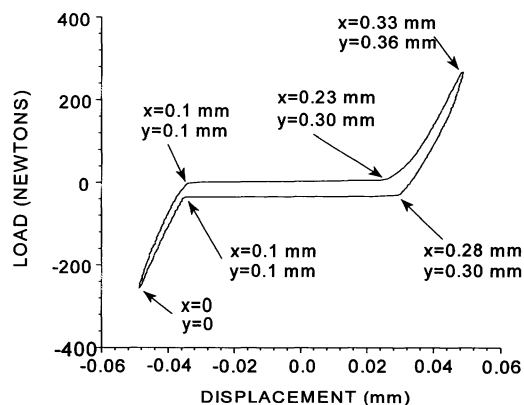


**FIGURE 10** Illustration of the joint movement in off axis directions.

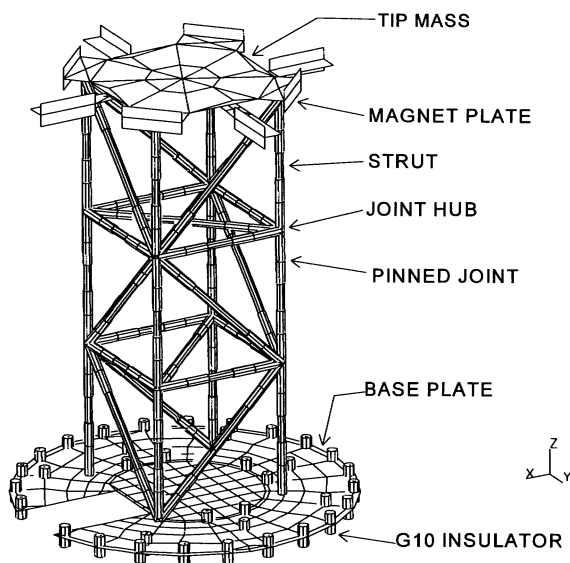


**FIGURE 11** Illustration of three bay truss finite element model.

the strut loss factors, the fraction of strain energy in each strut was needed. A finite element model of the entire truss (see Fig. 11) was created and used to find those strain energy terms. A loss factor was then predicted for the truss with locked and unlocked joints using the locked and unlocked strut loss factors from the 4.737-mm pin test. Equation (2) predicts an unlocked truss loss factor of 0.072 for a strut loss factor of 0.20 (typical of a 4.737-mm pin). For a locked truss, eq. (2) predicts a loss factor of 0.032 for a strut loss factor of 0.033. Figure 12 shows a comparison

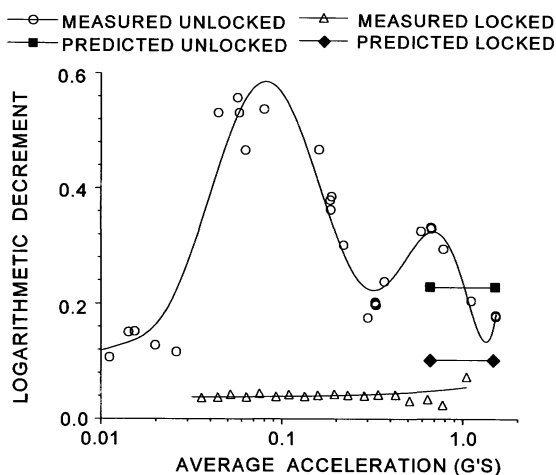


**FIGURE 12** Comparison of measured to predicted values for three bay truss.

son with the truss logarithmic decrement data, using eq. (4) to convert from loss factor to logarithmic decrement. The  $\pm 267$ -N load cycle used to measure the hysteresis loops would be consistent with a 1.3-g average acceleration level. Thus, Figure 12 only displays the predicted values near an acceleration of 1-g. Comparing measured and predicted values for the truss with unlocked joints shows general agreement. The predicted values for the locked truss are high compared with measured values. The damping predicted in the locked truss is sufficiently small ( $\eta = 0.032$  compared with the previously mentioned lower limit of 0.01) that the accuracy of the measurements is in question.

## CONCLUSIONS

Developing a method for characterizing joints was more difficult than expected. Although the testing process appears to be very straightforward, the test setup is very sensitive to small variations in the procedures. The setup was calibrated using a section of aluminum tubing with known stiffness and near zero hysteresis characteristics. A good match between expected and measured stiffness was achieved that provides increased confidence in the method used. The hysteresis tests of struts with pinned joints showed consistent trends in loss factor as a function of joint gap size. As larger pins were inserted in the strut joint, the joint gap decreased as well as the hysteresis loop size and loss factors. The tests were very successful in providing quasi-static stiffness characteristics of the struts.

All of the information gained from the characterization of joint hysteresis is essential to improving analytical models of the truss. These models will need to simulate the deadband, friction, and stiffness characteristics provided by the above tests.

It is not expected that the hysteresis tests should provide a comprehensive method for measurement of joint damping. These quasistatic tests do not simulate the important dynamic phenomena occurring in the motion of the struts. However, the results presented here provided a much better than expected correlation between measured and predicted values of damping for the three bay truss. A larger data base of predicted and measured values is required before a conclusion can be determined. A clear correlation between damping predicted from hysteresis

measurements and measured damping is not evident at this time.

## REFERENCES

- Crawley, E. F., Sigler, J. L., and van Schoor, M. C., 1988, "Hybrid Scaled Structural Models and Their Use in Damping Prediction," *AIAA Journal of Guidance, Control, and Dynamics*, Vol. 13, pp. 1023–1032.
- Folkman, S. L., and Redd, F. J., 1990, "Gravity Effects on Damping of a Space Structure with Pinned Joints," *AIAA Journal of Guidance, Control, and Dynamics*, Vol. 13, pp. 228–233.
- Hayasaka, Y., Okamoto, N., Hattori, T., et al., 1992, "Analysis of Nonlinear Vibration of Space Apparatuses Connected with Pin-Joints," *Transactions of the Japan Society of Mechanical Engineers, Part C*, Vol. 59, No. 563, pp. 41–48.
- Hutton, D. V., 1981, *Applied Mechanical Vibrations*, McGraw-Hill Book Company, New York.
- Masters, B. P., and Crawley, E. F., 1993, "Multiple Degree of Freedom Force-State Component Identification," *The 34th AIAA/ASME/ASCE/AHS/ASC Structures, Dynamics, and Materials Conference*, LaJolla, California, April 19–22, 1993, AIAA-93-1654-CP.
- Peebles, J. H., and Kempster, K. B., 1988, "Space Station Erectable Truss Joint Evaluation," *AIAA SDM Issues of the International Space Station*, Williamsburg, VA, April 21–22, 1988.
- Plunkett, R., 1980, "Friction Damping," in P. J. Torvik, *Damping Applications for Vibration Control*, American Society of Mechanical Engineers, New York, pp. 65–74.
- Steidel, R. F., 1971, *An Introduction to Mechanical Vibrations*, 3rd ed., John Wiley & Sons, New York.



**Hindawi**

Submit your manuscripts at  
<http://www.hindawi.com>

